

Journal Pre-proof

Doble Role Of Bathocuproine Disulfonic Acid As Multi-Walled Carbon Nanotubes Dispersing Agent And Copper Preconcentration Ligand: Analytical Applications For The Development Of Hydrogen Peroxide And Glucose Electrochemical Sensors



Pablo Gallay, Marcela Rodríguez, Marcos Eguilaz, Gustavo Rivas

PII: S0731-7085(20)31412-6
DOI: <https://doi.org/10.1016/j.jpba.2020.113526>
Reference: PBA 113526

To appear in: *Journal of Pharmaceutical and Biomedical Analysis*

Received Date: 2 July 2020
Revised Date: 31 July 2020
Accepted Date: 2 August 2020

Please cite this article as: Gallay P, Rodríguez M, Eguilaz M, Rivas G, Doble Role Of Bathocuproine Disulfonic Acid As Multi-Walled Carbon Nanotubes Dispersing Agent And Copper Preconcentration Ligand: Analytical Applications For The Development Of Hydrogen Peroxide And Glucose Electrochemical Sensors, *Journal of Pharmaceutical and Biomedical Analysis* (2020), doi: <https://doi.org/10.1016/j.jpba.2020.113526>

This is a PDF file of an article that has undergone enhancements after acceptance, such as the addition of a cover page and metadata, and formatting for readability, but it is not yet the definitive version of record. This version will undergo additional copyediting, typesetting and review before it is published in its final form, but we are providing this version to give early visibility of the article. Please note that, during the production process, errors may be discovered which could affect the content, and all legal disclaimers that apply to the journal pertain.

© 2020 Published by Elsevier.

DOBLE ROLE OF BATHOCUPROINE DISULFONIC ACID AS MULTI-WALLED CARBON NANOTUBES DISPERSING AGENT AND COPPER PRECONCENTRATION LIGAND: ANALYTICAL APPLICATIONS FOR THE DEVELOPMENT OF HYDROGEN PEROXIDE AND GLUCOSE ELECTROCHEMICAL SENSORS

Pablo Gallay, Marcela Rodríguez, Marcos Eguílaz,* Gustavo Rivas* grivas@fcq.unc.edu.ar

¹INFIQC. Departamento de Físicoquímica. Facultad de Ciencias Químicas. Ciudad Universitaria. 5000 Córdoba. Argentina.

***Corresponding author**

e-mail:; mrubio@fcq.unc.edu.ar;

Phone number: +54-351-4334169/80; Fax number: +54-351-4334188.

Highlights-RIVAS ET AL

- BCS presents the double role of exfoliating MWCNTs and accumulating Cu.
- The nanohybrid MWCNTs-BCS was successfully used to accumulate Cu in a robust way.
- GCE/MWCNTs-BCS/Cu makes possible the sensitive quantification of H₂O₂.

- GCE/MWCNT-BCS/Cu/GOx/Naf is successfully used to quantify glucose in milk and beverages.

ABSTRACT

We are reporting a new strategy for preparing carbon nanotubes (CNTs)-based hydrogen peroxide and glucose amperometric sensors by taking advantage of the dual role of bathocuproine disulfonic acid (BCS) as dispersing agent of multi-walled carbon nanotubes (MWCNTs) and as ligand for the preconcentration of Cu(II). The platform was obtained by casting glassy carbon electrodes (GCE) with the dispersion of MWCNTs in BCS (MWCNTs-BCS) followed by the preconcentration of Cu(II) by surface complex formation at open circuit potential (GCE/MWCNTs-BCS/Cu). The resulting electrode was used for the sensitive amperometric quantification of hydrogen peroxide at 0.400 V catalyzed by the preconcentrated copper, with a linear range between 5.0×10^{-7} and 7.4×10^{-6} M, a sensitivity of $24.3 \text{ mA} \cdot \text{M}^{-1}$, and a detection limit of $0.2 \text{ } \mu\text{M}$. The adsorption of GOx at GCE/MWCNTs-BCS/Cu followed by the immobilization of Nafion (Naf), allowed the construction of a sensitive and selective amperometric glucose biosensor with a linear range between 5.0×10^{-6} M and 4.9×10^{-4} M, a sensitivity of $(477 \pm 3) \text{ } \mu\text{A} \cdot \text{M}^{-1}$ and a detection limit of $2 \text{ } \mu\text{M}$. The proposed (bio)sensors were successfully used for the quantification of hydrogen peroxide in enriched milk samples and glucose in milk and commercial beverages without any pretreatment.

Keywords: Carbon nanotubes; Bathocuproine disulfonic acid; Copper; Hydrogen peroxide electrochemical sensor; Glucose electrochemical biosensor.

1. INTRODUCTION

Nanomaterials have played a key role in the development of electrochemical (bio)sensors due to their multiple advantages to build (bio)analytical platforms and improve the transduction of (bio)recognition events [1-3]. Particularly, the use of carbon nanotubes (CNTs) for the development of electrochemical sensors, have demonstrated to be a highly successful strategy due to their well-known properties mainly connected with the large surface area, good conductivity, catalytic activity towards the oxidation/reduction of different analytes, and multiple possibilities of functionalization [4, 5]. However, despite these unique properties, CNTs require a functionalization step to disaggregate the bundles before the incorporation in the electrochemical sensors [6]. This functionalization, either covalent or non-covalent, has two main goals, the obvious one, to exfoliate the nanostructures and allow their dispersion in aqueous media, and the other one, more challenging, to give particular properties to the disaggregated nanostructures [7]. In fact, depending on the nature of the dispersing agents, these properties can be connected to special groups and/or to the biorecognition ability that will allow the anchoring/preconcentration of diverse species and the direct biosensing/bioaffinity interaction, respectively [7].

Different strategies have been proposed for de-bundling and functionalizing CNTs, using ionic liquids, polymers, biomolecules, organic molecules and eutectic mixtures, among others [8, 9]. Polymers like polyhistidine, polylysine [7], polyarginine [10], polytyrosine [11], small biomolecules like cysteine [12], and biomacromolecules such as glucose oxidase [13], cytochrome c [14], calf-thymus double stranded DNA (dsDNA) [15], avidin [16] and concanavalin A [17] have been successfully used for disaggregating the MWCNTs and building different (bio)sensors.

Hydrogen peroxide is a very important analyte that is receiving increasing attention due to the connection with important metabolic routes, the importance in different industries, the significance as biomarker of diverse pathologies mainly associated with cancer and degenerative processes [18], and its widespread use as indicator for transducing different biorecognition events [19]. In this sense, the most typical example is the use of hydrogen peroxide as indicator for glucose oxidase (GOx)-based first generation electrochemical glucose biosensors. Considering that the oxidation and reduction of hydrogen peroxide at carbon electrodes require elevated overvoltages [20], different strategies have been used to overcome this problem. Among them, the incorporation of transition metal nano/micro-particles, like Cu [21], Au [22], Ir [23], Pd [24], Rh [25], Ru [26], and alloys like Cu@PtPd/C [27] core-shell nanoparticles, has demonstrated to be highly successful due to the catalytic activity of these metals for the oxidation and reduction of hydrogen peroxide.

Recently [28], we have reported an electrochemical sensor for the highly sensitive and selective quantification of Cu(II) through the use of MWCNTs non-covalently functionalized with bathocuproine disulfonic acid (BCS), a compound

analogue to the ligand bathocuproine (BC), that is an excellent ligand for complexing Cu(I) (Cu(I)-BCS, $\log \beta = 19.8$) and Cu(II) (Cu(II)-BCS $\log \beta_2 = 11.9$) [29, 30].

Here, we propose the use of GCE modified with MWCNTs non-covalently functionalized with BCS as Cu(II)-preconcentration layer (GCE/MWCNTs-BCS/Cu) for the development of hydrogen peroxide sensors and glucose biosensors previous incorporation of glucose oxidase (GOx), based on the catalytic activity of the accumulated copper on hydrogen peroxide oxidation. In the following sections we discuss the optimization of the preparation conditions for GCE/MWCNTs-BCS/Cu, the construction of the glucose biosensor and the analytical performance of the resulting bioanalytical platforms for the quantification of hydrogen peroxide and glucose.

2. MATERIALS AND METHODS

2.1. Chemicals and solutions

Carbon nanotubes (MWCNTs, (30 ± 15) nm diameter, $(1-5)$ μm length and 95.5 % purity, bathocuproine disulfonic acid disodium salt (BCS), glucose, lactose, fructose, galactose, maltose, glucose oxidase from *Aspergillus niger* EC 1.1.3.4 163,400 units/g of solid)), copper atomic absorption standard solution ($1010 \mu\text{g.mL}^{-1}$ in 5 % HCl) and Nafion (Naf) were

supplied from Sigma-Aldrich. Hydrogen peroxide was acquired from Carlo Erba. Other chemicals were of analytical grade and used without further purification.

A 0.050 M phosphate buffer solution pH 7.40 was used as supporting electrolyte. Ultrapure water ($\rho = 18.2 \text{ M}\Omega \text{ cm}$) from a Millipore-MilliQ system was used for preparing all aqueous solutions.

2.2. Apparatus

Ultra-sonication was carried out with an ultrasonic processor VCX 130W, Sonics and Materials, Inc. of 20 kHz frequency with a microtip of titanium alloy of 3 mm-diameter.

Electrochemical experiments were performed with a TEQ_04 potentiostat. Glassy carbon electrodes (GCE, CH Instruments, 3mm-diameter) modified with MWCNTs dispersed in BCS containing the preconcentrated Cu(II) (GCE/MWCNTs-BCS/Cu) and GCE/MWCNTs-BCS/Cu modified with GOx and Naf (GCE/MWCNTs-BCS/Cu/GOx/Naf) were used as working electrodes. A Pt wire and Ag/AgCl, 3 M NaCl (BAS) were used as auxiliary and reference electrodes, respectively. All potentials are referred to this reference electrode.

Scanning Electron Microscopy (SEM) images were obtained with a Field Emission Gun Scanning Electron Microscope (FE-SEM, Zeiss, SIGMA model) equipped with secondary and back-scattered electron detectors. The samples

were prepared by drop-coating of the MWCNT-BCS dispersion onto GCE disks followed by the accumulation of Cu(II) at open circuit potential previous evaporation of the solvent at room temperature.

2.3. Preparation of the modified electrodes

2.3.1. Preparation of GCE modified with MWCNTs-BCS and Cu (GCE/MWCNTs-BCS/Cu): this electrode was prepared according to reference [28]. Briefly, MWCNTs (0.5 mg mL^{-1}) were dispersed in 1.0 mg mL^{-1} BCS using a sonicator probe with amplitude of 50% for 10 min while keeping in an ice-bath. GCE/MWCNTs-BCS was obtained by casting $10 \text{ }\mu\text{L}$ of MWCNTs-BCS on the top of GCE previously polished with alumina slurries of 1.0, 0.3 and $0.05 \text{ }\mu\text{m}$, rinsed thoroughly with deionized water, sonicated for 30 s in water, and finally dried under a N_2 stream. The preconcentration of Cu was performed at open circuit potential (ocp) by immersion of GCE/MWCNTs-BCS in a 2.5 ppm Cu(II) solution prepared in 0.020 M acetate buffer solution pH 5.00 for 3.0 min under stirring conditions.

2.3.2. Preparation of GCE/MWCNTs-BCS/Cu modified with GOx and Naf (GCE/MWCNTs-BCS/Cu/GOx/Naf): the biosensor was prepared by drop-coating 2.0 mg mL^{-1} GOx onto GCE/MWCNTs-BCS/Cu, followed by the deposition of $5 \text{ }\mu\text{L}$ of 0.5 % w/v Naf. Figure 1 shows the scheme for the preparation of the different platforms.

2.4. Procedure

The quantification of hydrogen peroxide and glucose was performed by amperometry at 0.400 V. All electrochemical experiments were conducted at room temperature in a 0.050 M phosphate buffer solution pH 7.40.

Hydrogen peroxide was quantified in a milk sample (La Serenisima®) enriched with 1.7×10^{-3} M hydrogen peroxide by transferring a given aliquot of the milk enriched sample to the electrochemical cell containing 5.0 mL of 0.050 M phosphate buffer solution pH 7.40, performing the quantification by amperometry at 0.400 V using GCE/MWCNTs-BCS/Cu.

Glucose was quantified in milk (La Serenisima®) and two commercial drinks, Gatorade® and Red-Bull®. The beverages and milk were obtained from a local supermarket. An aliquot of the given sample was directly transferred to the electrochemical cell containing 5.0 mL of 0.050 M phosphate buffer pH 7.40 and the determination of glucose was carried out by amperometry at 0.400 V at GCE/MWCNTs-BCS/Cu/GOx/Naf biosensor using the standard addition method in the three cases.

3. RESULTS AND DISCUSSION

3.1. Characterization of GCE/MWCNTs-BCS/Cu

Figure 2A shows SEM pictures of GCE/MWCNTs-BCS/Cu prepared by modification of GCE with a dispersion of 0.50 mgmL⁻¹ MWCNTs in 1.0 mg mL⁻¹ BCS, followed by the preconcentration of Cu (II) by immersion in a 2.5 ppm Cu (II) solution

for 3.0 min at ocp. The whole surface of the glassy carbon disk is covered by MWCNTs-BCS although, in agreement with the pattern obtained for other MWCNTs-modified GCEs [7] there are areas with different density of MWCNTs. As it was previously demonstrated [28], BCS largely contributes to the exfoliation of MWCNTs due the facilitated interaction with the aqueous solvent through the sulfonate groups of the BCS that supports the MWCNTs. The EDX map of the glassy carbon disk shown in Figure 2A (GCE/MWCNTs-BCS/Cu), demonstrates that copper is distributed in the whole surface, confirming the efficient preconcentration of Cu(II) at GCE/MWCNTs-BCS (Figure 2B).

Figure 2C displays the cyclic voltammetric profiles of GCE/MWCNTs-BCS (black line) and GCE/MWCNTs-BCS/Cu (red line) in a 0.050 M phosphate buffer solution pH 7.40. No peaks are observed at GCE/MWCNTs-BCS, while in the presence of Cu at the electrode surface, there are two anodic peaks due to the oxidation of Cu to Cu(I) (0.194 V) and Cu(I) to Cu(II) (0.416 V). The corresponding reduction of Cu(II) to Cu(I) is observed at 0.407 V, while the reduction of Cu(I) to Cu mostly occurs at potentials close to 0 V. Successive voltammograms performed with GCE/MWCNTs-BCS/Cu in buffer solution did not show significant differences in the peak currents for the oxidation and reduction of Cu, clearly evidencing that BCS retains copper in a very robust way (not shown). Therefore, BCS successfully works in the double role of MWCNTs disaggregation agent and surface copper preconcentration element.

3.2. Analytical application of GCE/MWCNTs-BCS/Cu for the quantification of hydrogen peroxide

Figure 3A displays the potentiodynamic i-E profiles obtained at GCE/MWCNTs-BCS/Cu in a 0.050 M phosphate buffer solution pH 7.40 without (black line) and with (red line) 2.0×10^{-2} M hydrogen peroxide. The cyclic voltammogram obtained in the absence of hydrogen peroxide presents the expected profile according to Figure 2C. The voltammetric response for 2.0×10^{-2} M hydrogen peroxide shows a huge increment of the oxidation and reduction currents due to the catalytic activity of copper [21]. Figure 3B displays the hydrodynamic voltammograms for 2.0×10^{-4} M hydrogen peroxide at GCE/MWCNTs-BCS (black) and GCE/MWCNTs-BCS/Cu (red). In agreement with Figure 3A, the presence of copper at the electrode surface produces a drastic decrease in the overvoltages for the oxidation and reduction of hydrogen peroxide and a noticeable increment in the associated currents, confirming, once more, the excellent catalytic activity of the copper preconcentrated at the BCS that supports the MWCNTs.

The effect of the accumulation time of 2.5 ppm Cu(II) at GCE/MWCNTs-BCS on the sensitivity for the oxidation of hydrogen peroxide at 0.400 V is shown in Figure 4A. The sensitivity increases with the interaction time and reaches a maximum after 3.0 min, suggesting a saturation of the available sites of the BCS that supports the MWCNTs for complex formation. We also evaluated the influence of Cu(II) concentration used for the preconcentration at GCE/MWCNTs-BCS for 3.0 min on the sensitivity for hydrogen peroxide oxidation (Figure 4B). It increases with the concentration of Cu(II), reaching a maximum after 2.5 ppm Cu(II). Therefore, the selected conditions for the preconcentration of Cu at the surface of GCE/MWCNTs-BCS were an interaction time of 3.0 min at ocp using a 2.5 ppm Cu(II) solution.

The amperometric response of H_2O_2 at GCE/MWCNTs-BCS/Cu at a working potential of 0.400 V is displayed in Figure 5A. After the addition of H_2O_2 , the current rapidly increases and reaches the steady-state after 3 seconds. The inset shows the amperometric response for the lower concentrations range. The corresponding calibration plot is depicted in Figure 5B. The linear range goes from 5.0×10^{-7} M to 7.4×10^{-6} M, with a sensitivity of $24.3 \text{ mA}\cdot\text{M}^{-1}$ ($r^2 = 0.990$), and a detection limit of $0.2 \text{ }\mu\text{M}$ (taken as $3.3 \sigma/S$, where σ is the blank signal-standard deviation and S the sensitivity). The reproducibility obtained for 5 electrodes modified with the same MWCNTs-BCS dispersion was 7.1 %.

Table 1-SI (Supplementary Information) compares the analytical performance of our H_2O_2 sensor with the most relevant non-enzymatic hydrogen peroxide amperometric sensors reported since 2017. The proposed H_2O_2 sensor possesses a competitive detection limit which is lower than those obtained in [1-6, 10, 12], comparable to those reported in the references [24, 7, 8, 11] and higher than those presented in [26, 9, 14]. However, even when the detection limit of the proposed sensor is higher than those reported in ref. [9, 14], is important to remark that, these sensors require a more complex and expensive preparation, either using GCE modified with MWCNTs-SnO₂ nanofibers, hemoglobin and chitosan [45] or CF@N-CNTAs-AuNPs [50]. In addition, the working potentials for these sensors [9, 14] are very negative (-0.40 and -0.30 V, respectively), making necessary the desoxygenation of the solution and longer times to stabilize the base line currents. GCE/MWCNTs-Av/Ru [26] was proposed recently by our group and allowed to reach detection limits three times smaller than GCE/MWCNTs-BCS/Cu, with a considerably wider linear range, although the sensitivity is comparable to that

of our sensor. One advantage of our sensor, is that the element responsible for the catalytic activity (Cu) is considerably cheaper than the one used in the case of GCE/MWCNTs-Av/Ru. In summary, the sensor proposed in this work is very competitive alternative compared to the already existing ones.

Figure 5C compares the sensitivity for hydrogen peroxide obtained from amperometric recordings at 0.400 V at GCE/MWCNTs-BCS and GCE/MWCNTs-BCS/Cu. As expected, the sensitivity for hydrogen peroxide obtained at GCE/MWCNTs-BTC is negligible compared to the one obtained at GCE/MWCNTs-BCS/Cu.

We evaluate the analytical application of the sensor, determining the recovery of hydrogen peroxide in a milk sample enriched with 1.7×10^{-3} M hydrogen peroxide, without any pre-treatment. The recovery percentage was $(94 \pm 9) \%$ demonstrating the analytical usefulness of the proposed sensor for the highly sensitive and selective quantification of hydrogen peroxide in untreated milk samples.

3.3. Analytical applications of GCE/MWCNTs-BCS/Cu/GOx/Naf for the quantification of glucose

Figure 6A displays the amperometric response of glucose at GCE/MWCNTs-BCS/Cu/GOx/Naf at 0.400 V. A well-defined and fast response is observed after each addition of glucose. The corresponding calibration plot, displayed in Figure 6B, shows a linear range between 1.0×10^{-5} M and 4.9×10^{-4} M, with a sensitivity of $(477 \pm 3) \mu\text{A M}^{-1}$ ($r^2 = 0.9996$), and a limit of detection of 2 μM (calculated as it was previously indicated).

Different concentrations of GOx and dilutions of Naf were evaluated and the best compromise between sensitivity, stability and reproducibility was obtained using 2.0 mg/mL GOx and 0.5 % w/v Naf (results not shown).

The reproducibility, obtained from the sensitivity of 5 biosensors, was 9.3% using the same MWCNTs-BCS dispersion. The selectivity of GCE/MWCNTs-BCS/Cu/GOx/Naf was evaluated in the presence of 1.0×10^{-4} M lactose, galactose, fructose and maltose. No interference was obtained for lactose and maltose, while for galactose and fructose it was just (7.7 ± 0.9) % and (7.2 ± 0.1) %, respectively, demonstrating the selectivity of the biosensor in the presence of other sugars.

Table 2-SI (Supplementary Information) summarizes the analytical performance of the most representative enzymatic glucose biosensors with electrochemical transduction reported since 2018. The detection limit of our biosensor is better than those reported in references [23-28, 31-33], comparable to the ones obtained in [17-22, 30] and higher than those reported in references [15, 16, 29, 34]. GCE/AuNF/GS-IL-AuNRs/GOx/GA/Naf [16], Pt/GOx/gelatin [29] and Pt/IrNPs/Ludox/GOx [34] involve expensive noble metals like Au, Pt, and Pt-Ir, respectively. Therefore, our biosensor represents a competitive bioanalytical platform for glucose quantification with a relatively simple procedure for the preparation of the bioanalytical platform.

The practical application of the biosensor was evaluated using milk (La Serenísima®) and two beverages (Gatorade® and Red Bull®). The average concentration of glucose in milk, obtained from 5 determinations, was (2.0 ± 0.1) g/100 mL, value that is in excellent agreement with the one reported by the company (1.9 g.mL^{-1}). The glucose contents in Gatorade

and Red Bull obtained with our biosensor were (2.5 ± 0.3) g/100 mL and (3.4 ± 0.3) g/100 mL, respectively, values that also show an excellent correlation with the reported values (2.3 g/100mL and 3.6 g/100 mL, respectively). These results confirmed the analytical usefulness of GCE/MWCNTs-BCS/Cu/GOx/Naf nanohybrid platform for the development of an efficient electrochemical glucose biosensor that demonstrate practical applicability for the quantification in several untreated samples.

4. CONCLUSIONS

The platforms proposed in this work represent a fast, easy-to-prepare, reproducible, sensitive and selective alternative to develop hydrogen peroxide and glucose sensors with very competitive analytical performance and interesting practical applications in untreated samples, without the requirement of sophisticated instruments or complicated protocols. These platforms are the result of an efficient integration of MWCNTs, that offer a large surface and the robustness for the efficient immobilization of BCS and GOx; BCS, that allows the disaggregation of the carbon nanostructures and the preconcentration of the catalyst; and Cu, that efficiently catalyzes the oxidation of hydrogen peroxide.

This strategy to build a biosensing platform can be considered a prototype for further developments of other (bio)sensors, either based on the catalytic activity of copper for building non-enzymatic sensors, or biosensors based on hydrogen peroxide-producing oxidases.

DECLARATION OF COMPETING INTEREST

On behalf of the authors of the manuscript “doble role of bathocuproine disulfonic acid as multi-walled carbon nanotubes dispersing agent and copper preconcentration ligand: analytical applications for the development of hydrogen peroxide and glucose electrochemical sensors” by Gallay, Rodríguez, Eguílaz and Rivas, I declare that there are no conflicts of interest.

Declaration of interests

☒ The authors declare that they have no known competing financial interests or personal relationships that could have appeared to influence the work reported in this paper.

ACKNOWLEDGEMENTS

Financial support from CONICET, ANPCyT, SECyT-UNC is gratefully acknowledged. P. G. acknowledges the fellowship to CONICET.

REFERENCES

- [1] K.E. Sapsford, W.R. Algar, L. Berti, K.B. Gemmill, B.J. Casey, E. Oh, M.H. Stewart, I.L. Medintz. Functionalizing Nanoparticles with Biological Molecules: Developing Chemistries that Facilitate Nanotechnology. Chem. Rev. 113 (2013) 1904–2074.

- [2] Alireza Sanati, Mahsa Jalali, Keyvan Raeissi, Fathallah Karimzadeh, Mahshid Kharaziha, Sahar Sadat Mahshid, Sara Mahshid. A review on recent advancements in electrochemical biosensing using carbonaceous nanomaterials. *Microchim. Acta* 186 (2019) 773.
- [3] Samiul Alim, Jaya Vejjayan, Mashitah M. Yusoff, A.K.M. Kafi. Recent uses of carbon nanotubes & gold nanoparticles in electrochemistry with application in biosensing: A review. *Biosens. and Bioelectronics* 121 (2018) 125–136.
- [4] Fahimeh Movahedifar, Somayeh Tajik, and Shohreh Jahani. A Review on the Effects of Introducing CNTs in the Modification Process of Electrochemical Sensors Hadi Beitollahi. *Electroanal.* 31 (2019) 1195 – 1203.
- [5] Rivas G.A., Rodríguez M.C., Rubianes M.D., Gutierrez F.A., Eguílaz M., Dalmasso P.R., Primo E.N., Tettamanti C., Ramírez M.L., Montemerlo A., Gallay P., Parrado C. Carbon nanotubes-based electrochemical (bio)sensors for biomarkers. *Appl. Mater. Today* 9 (2017) 566–588.
- [6] Elham Asadiana, Masoumeh Ghalkhanib, Saeed Shahrokhiana. Electrochemical sensing based on carbon nanoparticles: A review. *Sensors & Actuators: B. Chemical* 293 (2019) 183–209.
- [7] Primo E.N., Gutiérrez F.A., Luque G.L., Dalmasso P.R., Gasnier A., Jalit Y., Moreno M., Bracamonte M. V., Rubio M.E., Pedano M.L., Rodríguez M.C., Ferreyra N.F., Rubianes M.D., Bollo S., Rivas G.A. Comparative study of the electrochemical behavior and analytical applications of (bio)sensing platforms based on the use of multi-walled carbon nanotubes dispersed in different polymers. *Anal Chim. Acta* 805 (2013) 19–35.

- [8] Ali Abo-Hamad, Maan Hayyan, Mohammed AbdulHakim AlSaadi, Mohamed E.S. Mirghani, Mohd Ali Hashim. Functionalization of carbon nanotubes using eutectic mixtures: A promising route for enhanced aqueous dispersibility and electrochemical activity. *J. of Molecular Liquids* 297 (2020) 111919.
- [9] Syed Tayyab Raza Naqvi, Tahir Rasheed, Dilshad Hussain, Muhammad Najam ul Haq, Saadat Majeed, Sameera shafi, Nisar Ahmed., Rahat Nawaz Modification strategies for improving the solubility/dispersion of carbon nanotubes. *J. of Molecular Liquids* 297 (2020) 111919.
- [10] Alejandro Gutiérrez, Fabiana Gutierrez, Marcos Eguílaz, Concepción Parrado, Gustavo A. Rivas. Non-covalent functionalization of multi-wall carbon nanotubes with polyarginine: characterization and analytical applications for uric acid quantification. *Electroanal.* 30 (2018) 1416-1424.
- [16] Eguílaz, M., Gutierrez, F., González-Domínguez, J.M., Martínez, M.T., Rivas, G. Single-walled carbon nanotubes covalently functionalized with polytyrosine: A new material for the development of NADH-based biosensors. *Biosen. and Bioelectronics* 86 (2016) 308-314.
- [11] Gutierrez F.A., Gonzalez-Dominguez J.M., Ansón-Casaos A., Hernández-Ferrer J., Rubianes M.D., Martínez M.T., Rivas G. Single-walled carbon nanotubes covalently functionalized with cysteine: A new alternative for the highly sensitive and selective Cd(II) quantification. *Sensor Actuators B Chem.* 249 (2017) 506–514.

- [13] Gutierrez, F., Rubianes, M.D., Rivas, G.A. Dispersion of multi-wall carbon nanotubes in glucose oxidase: Characterization and analytical applications for glucose biosensing. *Sensors Actuators B Chem.* 161 (2012), 191–197.
- [14] Eguílaz, M., Gutiérrez, A., Rivas, G. Non-covalent functionalization of multi-walled carbon nanotubes with cytochrome c: Enhanced direct electron transfer and analytical applications. *Sensors and Actuators B: Chemical* 225 (2016) 74-80.
- [15] Primo, E.N., Oviedo, M.B., Sánchez, C.G., Rubianes, M.D., Rivas, G.A. Bioelectrochemical sensing of promethazine with bamboo-type multiwalled carbon nanotubes dispersed in calf-thymus double stranded DNA. *Bioelectrochemistry* 99 (2014) 8–16.
- [16] Gutierrez, F.A., Rubianes, M.D., Rivas, G.A. New bioanalytical platform based on the use of avidin for the successful exfoliation of multi-walled carbon nanotubes and the robust anchoring of biomolecules. Application for hydrogen peroxide biosensing. *Anal. Chim. Acta* 1065 (2019) 12–20.
- [17] Ortiz, E., Gallay, P., Galicia, L., Eguílaz, M., Rivas, G. Nanoarchitectures based on multi-walled carbon nanotubes non-covalently functionalized with Concanavalin A: A new building-block with supramolecular recognition properties for the development of electrochemical biosensors. *Sensors and Actuators B: Chemical* 292 (2019) 254-262.
- [18] Hamed Shamkhalichenar, Jin-Woo Choi. Review—Non-Enzymatic Hydrogen Peroxide Electrochemical Sensors Based on Reduced Graphene Oxide. *J. of The Electrochemical Society* 167 (2020) 037531.

- [19] Eguílaz M., Dalmasso P., Rubianes M., Gutierrez F., Rodríguez M., Gallay P., López Mujica M., Ramírez M., Tettamanti C., Montemerlo A., Rivas G. Recent advances in the development of electrochemical hydrogen peroxide carbon nanotube-based (bio) sensors. *Current Opinion in Electrochemistry* 14 (2019) 157-165.
- [20] Keerthy Dhara, Debiprosad Roy Mahapatra. Recent advances in electrochemical nonenzymatic hydrogen peroxide sensors based on nanomaterials: a review. *J. Mater Sci* 54 (2019) 12319–12357.
- [21] Rodriguez, M. C., Rivas, G. A. Highly selective first generation glucose biosensor based on carbon paste containing copper and glucose oxidase. *Electroanal.* 13 (2001) 1179-1184.
- [22] Celej M.S., Rivas G.A. Amperometric Glucose Biosensor Based on Gold-Dispersed Carbon Paste. *Electroanal.* 10 (1998) 771–775.
- [23] Wang J., Rivas G. and Chicharro M. Glucose microsensor based on electrochemical deposition of iridium and glucose oxidase onto carbon fiber electrodes. *J. of Electroanalytical Chemistry* 439 (1997) 55-61.
- [24] Huang, B., Wang, Y., Lu, Z., Du, H., & Ye, J. One pot synthesis of palladium-cobalt nanoparticles over carbon nanotubes as a sensitive non-enzymatic sensor for glucose and hydrogen peroxide detection. *Sensors and Actuators B: Chemical* 252 (2017) 1016-1025.
- [25] Highly Selective Membrane-Free, Mediator-Free Glucose Biosensor. Joseph. Wang, Jie. Liu, Liang. Chen, Fang. Lu, *Anal. Chem.* (1994) 66, 21, 3600–3603.

- [26] Gallay, P., Eguílaz, M., Rivas, G. Designing electrochemical interfaces based on nanohybrids of avidin functionalized-carbon nanotubes and ruthenium nanoparticles as peroxidase-like nanozyme with supramolecular recognition properties for site-specific anchoring of biotinylated residues. *Biosensors and Bioelectronics* 148 (2020) 111764.
- [27] Gutierrez F. A., Giordana I. S., Fuertes V. C., Montemerlo A., Sieben J. M., Alvarez A.E., Rubianes M. D., Rivas G. A. Analytical applications of Cu@PtPd/C nanoparticles for the quantification of hydrogen peroxide. *Microchemical Journal* 141 (2018) 240-246.
- [28] Saldaña J., Gallay P., Gutierrez, S., Eguílaz M., Rivas G. Multi-walled carbon nanotubes functionalized with bathocuproinedisulfonic acid: analytical applications for the quantification of Cu (II). *Analytical and Bioanalytical Chemistry* (2020) 1-8.
- [29] Chen D, Darabedian N, Li Z, Kai T, Jiang D, Zhou F. An improved Bathocuproine assay for accurate valence identification and quantification of copper bound by biomolecules. *Anal. Biochem.* 497 (2016) 27-35.
- [30] Gayathri P, Kumar AS. Electrochemical Behavior of the 1,10-Phenanthroline Ligand on a Multiwalled Carbon Nanotube Surface and Its Relevant Electrochemistry for Selective Recognition of Copper Ion and Hydrogen Peroxide Sensing. *Langmuir* 30 (2014) 10513–10521.

Journal Pre-proof

LEGENDS OF THE FIGURES

Figure 1: Schematic representation of the steps involved in the functionalization of MWCNTs with BCS and copper.

Figure 2: (A) SEM micrograph of a glassy carbon disk modified with a dispersion of 0.50 mg mL^{-1} MWCNTs in 1.0 mg mL^{-1} BCS, followed by the preconcentration of Cu (II) by immersion in a 2.5 ppm Cu (II) solution for 3.0 min at ocp. Magnification: $10,000 \times$ (B) EDX of the GCE/MWCNTs-BCS/Cu. C) Cyclic voltammograms obtained at GCE/MWCNTs-BCS (black) and at GCE/MWCNTs-BCS/Cu (red) in phosphate buffer solution 0.050 M pH 7.40 . Scan rate: 50 mV.s^{-1} . Modification of GCE: same conditions as in Figure 2A.

Figure 3: (A) Cyclic voltammograms obtained at GCE/MWCNTs-BCS/Cu in phosphate buffer solution 0.050 M pH 7.40 (black) and $2.0 \times 10^{-2} \text{ M H}_2\text{O}_2$ (—). Scan rate: 0.050 V s^{-1} . (B) Hydrodynamic voltammogram for $2.0 \times 10^{-4} \text{ M H}_2\text{O}_2$ at GCE/MWCNTs-BCS/Cu (black) and GCE/MWCNTs-BCS/Cu (red).

Figure 4: Sensitivities for hydrogen peroxide obtained from amperometric recordings at GCE/MWCNTs-BCS/Cu as a function of (A) the accumulation time and (B) Cu(II) concentration. Working potential: $+0.400 \text{ V}$. Supporting electrolyte: 0.050 M phosphate buffer solution pH 7.40 . Cu(II) concentration (A): 2.5 ppm . Accumulation time (B): 3.0 min .

Figure 5: (A) Amperometric recording obtained at GCE/MWCNTs-BCS/Cu for successive additions of 5.0×10^{-7} M (a), 1.0×10^{-6} M (b), 5.0×10^{-6} M (c), and 1.0×10^{-5} M (d) H_2O_2 . Inset: amperometric recording for the lower concentrations range. (B) Calibration plot obtained from the amperometric recording shown in Figure 5 A. Inset: calibration plot in a more restricted concentrations range. (C) Sensitivities for H_2O_2 obtained from amperometric experiments using GCE/MWCNTs-BCS and CGE/MWCNTs-BCS/Cu. Inset: amperometric recordings for successive additions of hydrogen peroxide at GCE/MWCNTs-BCS (black) and GCE/MWCNTs-BCS-Cu (red). Working potential: +0.400 V. Supporting electrolyte: 0.050 M phosphate buffer solution pH 7.40.

Figure 6: (A) Amperometric recording obtained at GCE/MWCNTs-BCS/Cu/GOx/Nf for successive additions of 1.0×10^{-5} M (a), 5.0×10^{-5} M (b), and 1.0×10^{-4} M (c) glucose. Inset: shows the amperometric recording for the lower concentrations range. (B) Calibration plot obtained from the amperometric recording shown in Figure 6 A. Inset: calibration plot in a more restricted concentrations range.

Table 1: Comparison of the analytical performance of GCE/MWCNTs-BCS/Cu with those of the the most relevant non-enzymatic electrochemical hydrogen peroxide sensors reported since 2017.

TABLE 1. Comparison of the analytical performance of GCE/MWCNTs-BCS/Cu with those of the most relevant non-enzymatic amperometric hydrogen peroxide sensors reported since 2017.

Platforms	Amperometry Potential/V	Linear range	Sensitivity	LOD μM	Ref.
GCE/MWCNTs-Av/Ru	-0.050	$(5.0 \times 10^{-7} - 1.75 \times 10^{-3})$ M	25 $\text{mA} \cdot \text{M}^{-1}$	0.065	Ref.26 manuscript
GCE /CuCo ₂ O ₄ (hollow microspheres)	-0.55	(10 μM -8.9 mM)	94.1 $\mu\text{A} \cdot \mu\text{M}^{-1} \cdot \text{cm}^{-2}$	3	[1]
ITO/ErGO/MOF-BTC-Cu	-0.30	(4-17334) μM	679.57 $\mu\text{A} \cdot \mu\text{M}^{-1} \cdot \text{cm}^{-2}$	0.44	[2]
GCE/CuO nanoflowers	-0.40	(5 μM -14.07 mM)	956.69 $\mu\text{A} \cdot \mu\text{M}^{-1} \cdot \text{cm}^{-2}$	0.85	[3]
GCE/3D CuO/Cu nanoflowers	+0.60	(2.0 μM -19.4 mM)	103 $\mu\text{A} \cdot \mu\text{M}^{-1} \cdot \text{cm}^{-2}$	2	[4]
GCE/CuONBs/f-MWCNTs	-0.30	(5 μM -10.5 mM)	1100 $\mu\text{A} \cdot \mu\text{M}^{-1} \cdot \text{cm}^{-2}$	0.78	[5]
CPE/CuFe ₂ O ₄ /RGO	-0.35	(2-200) μM	0.82 $\mu\text{A} \cdot \text{mM}^{-1}$	0.52	[6]

GCE/Cu ₂ O nanocubes/Ag-Au alloy	-0.20	(0.05-50.75) mM	0.14 mM.cm ⁻²	0.10	[7]
GCE/AgNLS-CuNPS	-0.40	(0.5 – 1015) μ M	6190 μ A. μ M ⁻¹ .cm ⁻²	0.095	[8]
GCE/SnO ₂ NFs/MWCNTs-Hb-CS	-0.40	(1.0 x10 ⁻⁶ – 1.4 x10 ⁻⁴) M	-	0.03	[9]
BiVO ₄ /TiO ₂ nanocomposite	0.50	(5-400) μ M	3014 μ A.mM ⁻¹	5	[10]
Au/PDA@NPGF	-0.13	(1-100) μ M	2.53 μ A. μ M ⁻¹ .cm ⁻²	0.1	[11]
GCE/MWCNTs-Nafion/bpy/Cu ⁺²	0.20	(1 x10 ⁻⁶ -1 x10 ⁻³) M	96 nA. μ M ⁻¹ .cm ⁻²	4.5	[12]
SPCE/MWCNTs-PtNPs	+030	(1.0 x10 ⁻⁵ -1.0 x10 ⁻⁴) M	142.8 μ A.mM ⁻¹ .cm ⁻²	10	[13]
GCE/Pd-Co-CNTs	-0.15	(1.0 x10 ⁻⁶ – 1.11 x10 ⁻³) M	101.71 μ A.mM ⁻¹	0.3	Ref [24] manuscript
CF@N-CNTAs-AuNPs dispersed	-0.30	Up to 4.3 x10 ⁻³ M	142 μ A.mM ⁻¹ .cm ⁻²	0.05	[14]
CGE/MWCNTs-BCS/Cu	+ 0.40	(5.0 x 10⁻⁷-7.4 x10⁻⁶) M	24.3 mA.M⁻¹	0.2 μM	This work

GCE: Carbon glassy electrode, MWCNTs: multi-walled carbon nanotubes, Av: Avidine, ITO: indium tin oxide, MOF: metal-organic framework, ErGO: electrochemically reduced graphene oxide, BTC: 1,3,5-benzene-tricarboxylate, CuONBs/f-MWCNTs: multi-walled carbon nanotubes covered by copper oxide nanoberryes, CPE: carbon paste electrode, RGO: reduced graphene oxide, AgNLS–CuNPs: copper nanoparticles decorated silver nanoleaves, SnO₂NFs: SnO₂ multiporous nanofiber, Hb: hemoglobin, CS: chitosan, PDA@NPGF: polydopamine functionalized self-supported nanoporous gold film, bpy: bipyridyl, SPCE: screen-printed carbon electrode, PtNPs: Pt nanoparticles, CNTs: carbon nanotubes, N-CNTs: nitrogen doped carbon nanotubes, AuNPs: gold nanoparticles, BCS: bathocuproine disulfonic acid disodium salt.

Table 2: Comparison of the analytical performance of GCE/MWCNTs-BCS/Cu/GOx/Naf with those of the the most relevant amperometric enzymatic glucose biosensors reported in the period 2018-2020.

Table 2. Comparison of the analytical performance of GCE/MWCNTs-BCS/Cu/GOx/Naf with those of the the most relevant amperometric enzymatic glucose biosensors reported in the period 2018-2020.

Platform	Detection potential V	Linear range	Sensitivity	DL μM	Ref
GCE/fMWCNTs-mPEG/IL/GOx/Naf	-0.270	(20-950) μM	---	0.2	[15]
GCE/AuNF/GS-IL-AuNRs/GOx/GA/Naf	-0.200	(1-764) μM	0.06408 $\mu\text{A.mM}^{-1}$	0.38	[16]
Au/AuNPs@PNE/GOx/PNE	+0.700	(0.003-3.43) mM	35.4 $\mu\text{A.mM}^{-1}.\text{cm}^{-2}$	1.34	[17]
LIG/PEDOT-PSS/Pd@Pt	+0.550	(0.003-9.2) mM (0.010 -9.2) mM	247.3 $\mu\text{A.mM}^{-1}.\text{cm}^{-2}$	3	[18]
EVA-CNT/HRP-GOx	+0.000	(0.1– up to 1.0) mM	270 $\mu\text{A.mM}^{-1}.\text{cm}^{-2}$	3	[19]
Au/CG/C@MWCNTs/PtNPs/GOx/Nafion	+0.500	(0.5 -13) mM	26.5 $\mu\text{A.mM}^{-1}.\text{cm}^{-2}$	1.3	[20]
GCE/Zn-MOF-74-rGO-PtNPs-GOx	+0.200	(0.006-6) mM	64.51 $\mu\text{A.mM}^{-1}.\text{cm}^{-2}$	1.8	[21]
GCE/BiOIwrinkles/ZnO-NR/Ni(foam)	+0.300	(0.01-3.25) mM	115.2 $\mu\text{A.mM}^{-1}.\text{cm}^{-2}$	2	[22]
CGE/GC-COOH/GOx	+0.500	up to 12 mM	9.7 $\mu\text{A.mM}^{-1}.\text{cm}^{-2}$	9.5	[23]
SPCE/MWCNTs-NH ₂ /rGO/PANI/AuNPs/GOx	+0.400	(1-10) mM	246 $\mu\text{A.mM}^{-1}.\text{cm}^{-2}$	63	[24]
Tougue depressor/epoxy/CNTs/GOx	+0.600	(0.1-6) mM	2.281 $\mu\text{A.mM}^{-1}.\text{cm}^{-2}$	9.01	[25]
SPCE/P3ABA/rGO/Pt/GOx	+0.500	(0.25-6.00) mM	22.01 $\mu\text{A.mM}^{-1}.\text{cm}^{-2}$	44.3	[26]
GCE/ERGO/MWCNT/PyBA-GOx	-0.400	(0.15-2.10) mM	7.8 $\mu\text{A.mM}^{-1}.\text{cm}^{-2}$	43.3	[27]
ITO/ZnONRs/AuNPs /GOx/Nafion	-0.500	(0.05 - 1.0) mM	14.53 $\mu\text{A.mM}^{-1}.\text{cm}^{-2}$	180	[28]
Pt/GOx/gelatin	+0.600	up to 1.8 mM	1.24 $\mu\text{A.mM}^{-1}$ 152 $\mu\text{A.mM}^{-1}.\text{cm}^{-2}$	0.5	[29]
CGE/TCNFs-GOx	-0.550	(0.013-10.5) mM	628.82 $\mu\text{A.mM}^{-1}.\text{cm}^{-2}$	3.7	[30]
SPCE/GNR-MnO ₂ /GOx/Naf	+0.500	(0.1-1.4) mM	56.32 $\mu\text{A.mM}^{-1}.\text{cm}^{-2}$	50	[31]
SPCE/ERGO/IL-CHO/GOx	-0.450	(0.05-2.4) mM	17.7 $\mu\text{A.mM}^{-1}.\text{cm}^{-2}$	17	[32]

Au/PANI/PAA-GOx/Cat	-0.300	up 1.6 mM	49.3 $\mu\text{A} \cdot \text{mM}^{-1} \cdot \text{cm}^{-2}$	26.5	[33]
Pt/IrNPs/Ludox/GOx	+0.700	(0.05-3.2) mM	106 $\text{mA} \cdot \text{M}^{-1} \cdot \text{cm}^{-2}$	0.1	[34]
GCE/MWCNTs-BCS/Cu/GOx/Naf	+ 0.40	(0.010-0.49) mM	477 $\mu\text{A} \cdot \text{M}^{-1}$	2	This work

GCE: carbon glassy electrode, fMWCNTs: carboxylic acid-functionalized multi-walled carbon nanotubes, mPEG: aminated polyethylene glycol, IL: ionic liquid, GOx: glucose oxidase, Naf: Nafion; AuNF: Au nanoflowers, GS-IL: ionic liquid modified-graphene sheets, AuNRs: Au nanorods, GA: glutaraldehyde; AuNPs: Au nanoparticles, PNE: polynorepinephrine, GOx: glucose oxidase; LIG: laser-induced graphene, PEDOT-PSS: poly (3, 4-ethylene dioxythiophene)-poly (styrene sulfonate), Pd@Pt: platinum and palladium nanoparticles; EVA: ethylene-vinyl acetate copolymer, CNT: carbon nanotubes, HRP: horseradish peroxidase; CG: chemical derived graphene, C@MWCNTs: carboxylic functionalized multi-walled carbon nanotubes, PtNPs: Pt nanoparticles; MOF-74: metal-organic frameworks, rGO: reduced graphene oxide; ZnO-NR: ZnO-nanorods; GC-COOH: carboxyl-chitosan-functionalized nitrogen-containing graphene; SPCE: screen-printed carbon electrode, MWCNT-NH₂: amine-terminated multi-walled carbon nanotubes, PANI: polyaniline; Tongue depressor/epoxy/CNTs/GOD; P3ABA: poly(3-aminobenzoic acid); ERGO: electrochemically reduced graphene oxide, MWCNT: multiwall carbon nanotubes, PyBA: 4-(pyrrole-1-yl) benzoic acid; ITO: indium tin oxide, ZnONRs: zinc oxide nanorods; TCNFs: Titanium carbide carbon nanofibers; GNR: Graphene nanoribbons; CHO: 3-(3-formyl-4-hydroxybenzyl)-3- methylimidazolium hexafluorophosphate); PAA: poly(acrylic acid), Cat: catalase; IrNPs: Ir nanoparticle, Ludox HS-40: colloidal silica; BCS: bathocuproine disulfonic acid disodium salt

Figure 1- Rivas et al.

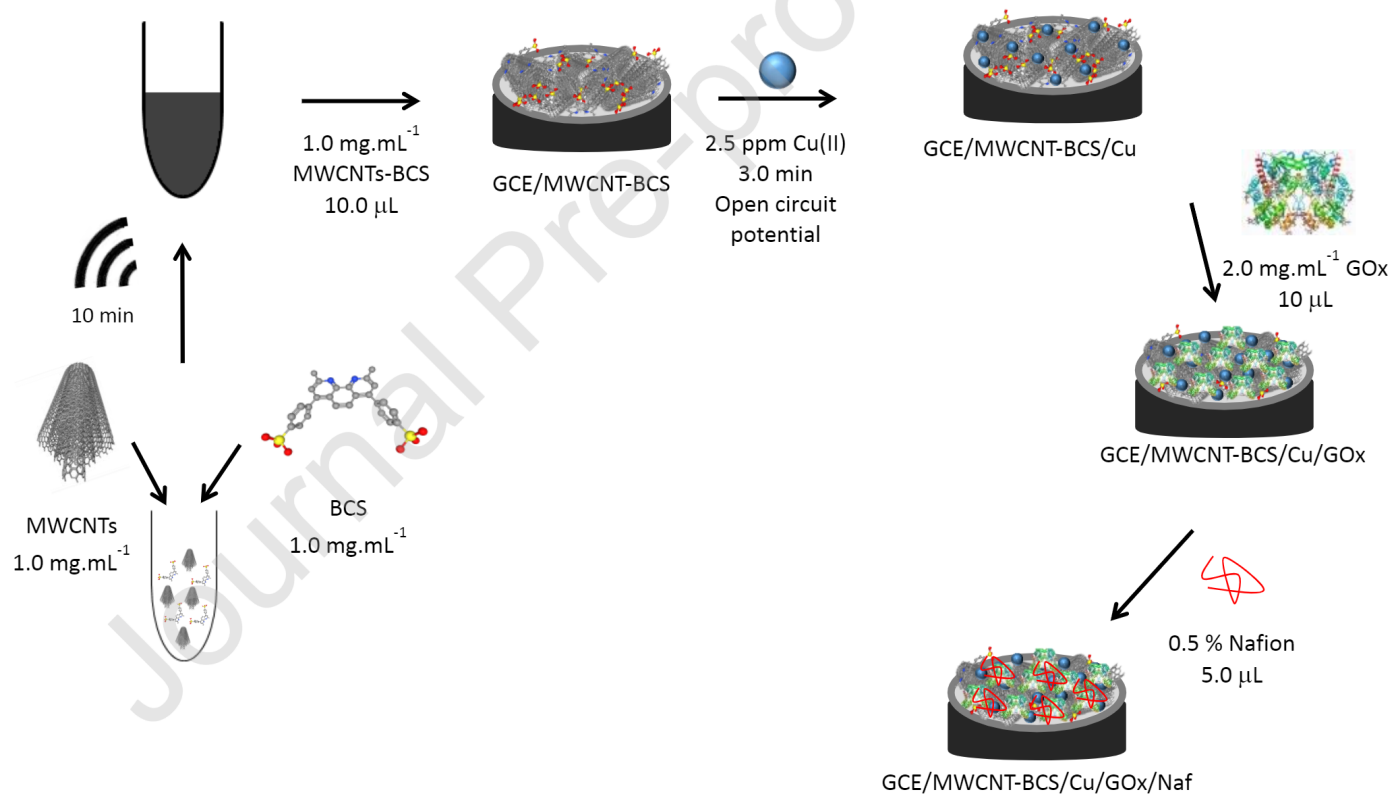


Figure 2- Rivas et al.

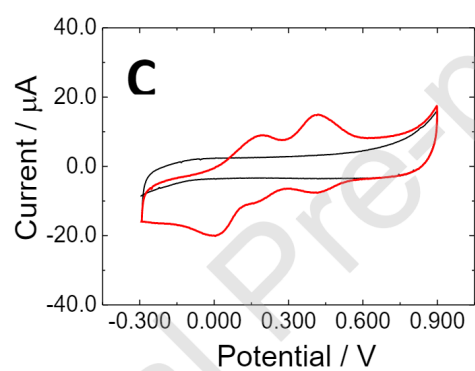
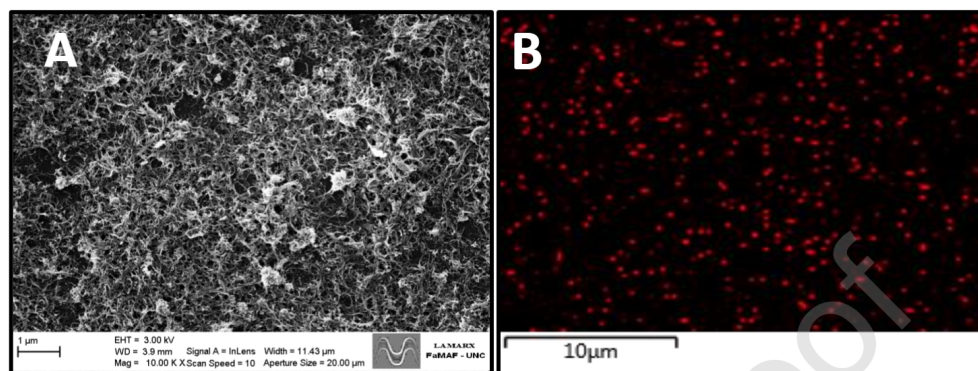


Figure 3- Rivas et al.

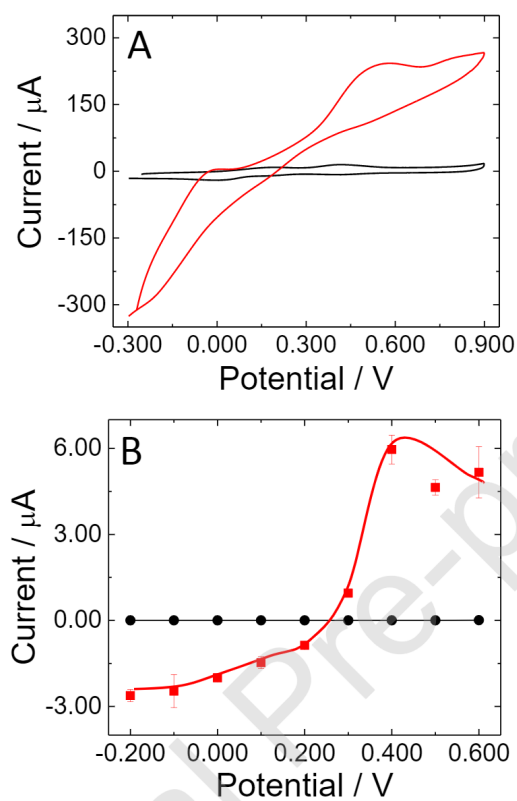


Figure 4 – Rivas et al.

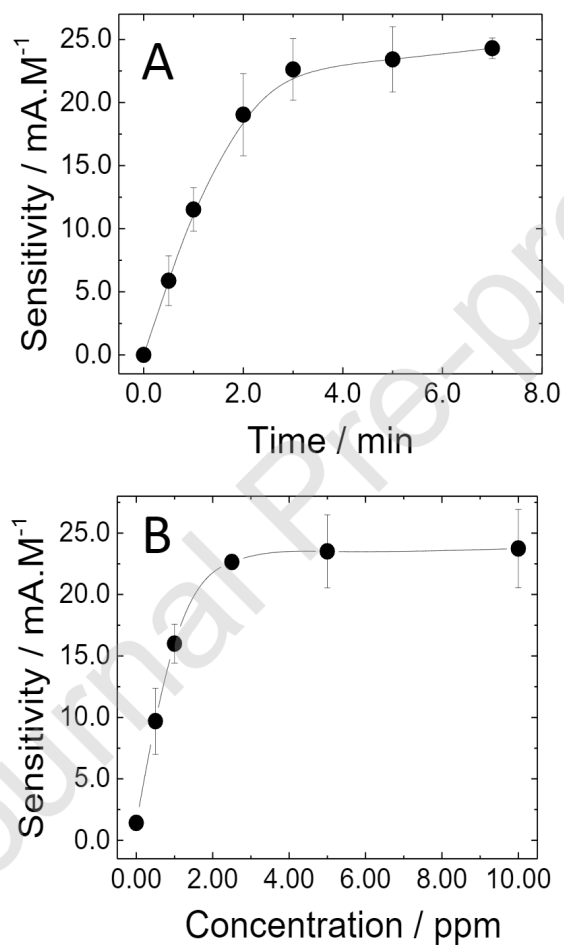


Figure 5 – Rivas et al.

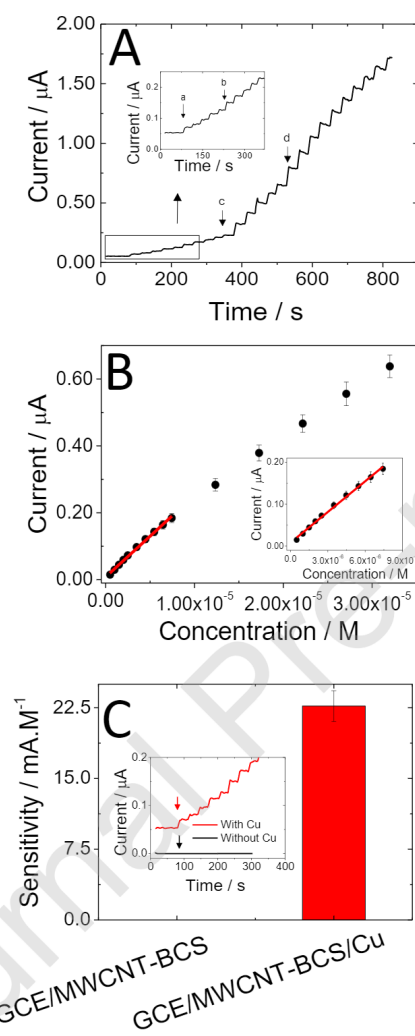


Figure 6- Rivas et al.

